

Entanglement concentration protocols for GHZ-type entangled coherent state based on linear optics

Mitali Sisodia^{1,*}; Chitra Shukla^{2,†}

¹ Indian Institute of Technology Jodhpur, Jodhpur, 342037 India

²Center for Quantum Computing, Peng Cheng Laboratory, Shenzhen 518055, People's Republic of China

Abstract

We proposed two entanglement concentration protocols (ECPs) to obtain maximally entangled Greenberger-Horne-Zeilinger (GHZ)-type entangled coherent state (ECS) from the corresponding partially entangled GHZ-type ECSs. We obtained the first ECP using a partially entangled GHZ-type ECS assisted with a superposition of single-mode coherent state, however the second ECP is designed using two copies of partially entangled GHZ-type ECSs. The success probabilities have also been calculated and discussed for both the ECPs. We have further compared the success probabilities of our first ECP for 3-mode GHZ-type ECS with an ECP of 3-mode W-type ECS and found that our ECP is more efficient (maximal success probabilities) for larger value ($\beta = 0.7$) of state parameter. For the physical realization, two optical circuits (for two ECPs) using linear optical elements, viz 50:50 beam splitter, phase shifter, and photon detectors are provided, which support the future experimental implementation possible with the present technology.

Keywords: Maximally entangled state, Entanglement concentration, GHZ-type entangled coherent state

1 Introduction

The robust quantum entanglement among the distant communicating parties is the backbone for any realization of the quantum information tasks like quantum teleportation [1], dense coding [2], quantum key distribution [3], quantum key agreement [4,5], quantum secret sharing [6], hierarchical quantum communication [7–9] and quantum secure direct communication [10, 11]. The sharing of maximal entanglement plays a key role in the success of the above applications to be performed deterministically [12]. In reality, the entanglement is generated locally and then distributed (shared) among the communicating users located remotely. Unfortunately, while transmission, manipulation and storage process, the entangled quantum systems undergo the interaction with an unavoidable noisy environment and hereof experience the degradation in maximal entanglement which lead to the probabilistic communication [13]. Therefore, a maximally entangled state (MES) will be turned into a less (partial) entangled state or even a mixed state thereby reduced (less than unity) teleportation fidelity would be obtained, which not only puts the security of quantum communication/computation [14] tasks at a high risk but also limits the distance of entanglement distribution. To overcome such serious problems, two prevalent approaches have been proposed to convert a non-MES into a MES in order to achieve the unit teleportation fidelity for the successful performance of the quantum information processing tasks. They are named as entanglement concentration protocol (ECP) and entanglement purification protocol (EPP). The ECP is considered for achieving the desired MES out of an ensemble of pure non-MESs whereas EPP is to obtain a high quality entangled states from the corresponding mixed states. In 1996, the first ECP has been proposed by Bennett et al. based on Schmidt decomposition [15]. Afterwards, several ECPs have been reported for different quantum states [16–25] [and references therein].

A Greenberger-Horne-Zeilinger (GHZ) state [26] is one of the important quantum entangled state among them. Along with the state generation [27, 28], GHZ state has been popular for the realization of various applications [29–31] in discrete variable (DV) domain where the entanglement is encoded in polarization of photons. For the perfect execution of such GHZ state applications numerous ECPs have also been introduced recently [24, 32–34] [and references therein]. Interestingly, in the similar way, GHZ state also has its significant importance in continuous variable (CV) domain where the entanglement is

*mitalisodiyadc@gmail.com;

†Corresponding Author: shuklac@pcl.ac.cn; chitrashukla07@gmail.com

encoded in superposition of coherent states $|\pm\alpha\rangle$ (α being amplitude with large values). Specifically, much attention has been given to continuous variable states in theory [35, 36] and experimental preparations [37, 38] due to their quantum nonlocality and high capacity. Practically, the CV states are superior as they overcome the limitations govern by DV states, such as low detection efficiency, high cost, and some limitations related to preparation and manipulation.

Therefore, beyond the conventional approach of using DV, the CV states have been of high interest among the researchers in recent years. Entangled coherent state (ECS) is a type of CV state that has attracted a lot of attention [35, 36]. Further, among the generation of various ECSs (in theory and experiment) like W-type ECS [39], Cluster-type ECS [37, 38, 40], the generation schemes of GHZ-type ECS have also been put forward in theory and experiment [37, 39]. Moreover, many applications in quantum communication [40, 41] using Cluster-type ECS, quantum cryptography using two-mode squeezed states [42], quantum teleportation using 3-mode ECS [43, 44] and quantum key distribution using GHZ-type ECS [45], quantum computation [46, 47] using Cluster-type ECS and quantum information processing tasks [48] using W-type ECS [49] have been proposed so far, that have reflected the significance of ECSs [37–40] and motivated the recently reported CV-based ECPs [50–52] (and references therein), too. In particular, Sheng et al. proposed ECP for Bell-type ECS [50] and W-type ECS [51]. Subsequently, Mitali et al. [52] designed two ECPs for Cluster-type ECS based on linear optics. Independently, the hybrid ECPs have also attracted the recent interest of the researchers [53, 54]. However, yet no ECP has been designed specifically for GHZ-type ECS. In fact, several applications have been proposed exploiting the GHZ-type ECS such as quantum teleportation [43, 44], quantum key distribution [45], very recently two communication schemes for controlled versions of quantum teleportation [55] and entanglement diversion [56]. It would be apt to note that with the recent progress of applications in quantum communication and cryptography [43–45, 55, 56], it is natural that the ECP has been in demand for GHZ-type ECS. Hence, designing ECPs for this state would be worth and of practical interest for the experimental implementation of these applications [55, 56] and as well as for more potential applications based on GHZ-type ECS. With this motivation, here we aim to propose two ECPs for 3-mode GHZ-type ECS, and to the best of our knowledge these ECPs have been the first attempt for 3-mode GHZ-type ECS.

The rest of the paper is organized as follows. In Sec. 2, we have described our proposed ECP for 3-mode GHZ-type ECS with the help of ancillary single-mode coherent state. Further, in Sec. 3 our next ECP has been discussed which uses two copies of 3-mode GHZ-type ECSs. Subsequently in Sec. 4, the success probabilities have been calculated and their corresponding plot has been shown in Fig. 3. Finally, the work has been concluded in the end in Sec. 5.

2 ECP for partially entangled 3-mode GHZ-type ECS with the help of a superposition of single-mode coherent state

A maximally entangled 3-mode GHZ-type ECS can be expressed as

$$|\Psi\rangle_{abc} = N_0 [|\alpha\rangle_a |\alpha\rangle_b |\alpha\rangle_c + |-\alpha\rangle_a |-\alpha\rangle_b |-\alpha\rangle_c], \quad (1)$$

where $N_0 = [2(1 + 2e^{-6|\alpha|^2})]^{-\frac{1}{2}}$ is the normalization coefficient. $|\pm\alpha\rangle$ are the coherent states and α is the amplitude with large values. The subscripts a , b and c represents the states possessed by Alice, Bob and Charlie, respectively.

Let us suppose, while sharing/distribution (to perform an application) of a , b and c modes, Eq. 1 gets transformed to a non-maximally ECS of the form

$$|\Psi'\rangle_{abc} = N_1 [\beta|\alpha\rangle_a |\alpha\rangle_b |\alpha\rangle_c + \gamma|-\alpha\rangle_a |-\alpha\rangle_b |-\alpha\rangle_c], \quad (2)$$

where $N_1 = [\beta^2 + \gamma^2 + 2\beta\gamma e^{-6|\alpha|^2}]^{-\frac{1}{2}}$ is the normalization coefficient. Here, β and γ are the probability amplitudes considered to be real numbers. In what follows, we aim to achieve a maximally entangled 3-mode GHZ-type ECS (1) from Eq. 2. To do so, we perform ECP as shown in Fig. 1, where Alice, Bob and Charlie share the non-maximally entangled ECS denoted in Eq. 2. In this ECP, first Charlie prepares a superposition of single-mode coherent state in the spatial mode d which can be expressed as

$$|\Phi\rangle_d = N_2 [\gamma|\alpha\rangle_d + \beta|-\alpha\rangle_d], \quad (3)$$

where, $N_2 = [\beta^2 + \gamma^2 + 2\beta\gamma e^{-2|\alpha|^2}]^{-\frac{1}{2}}$ is the normalization coefficient. Now, the combined state can be written as

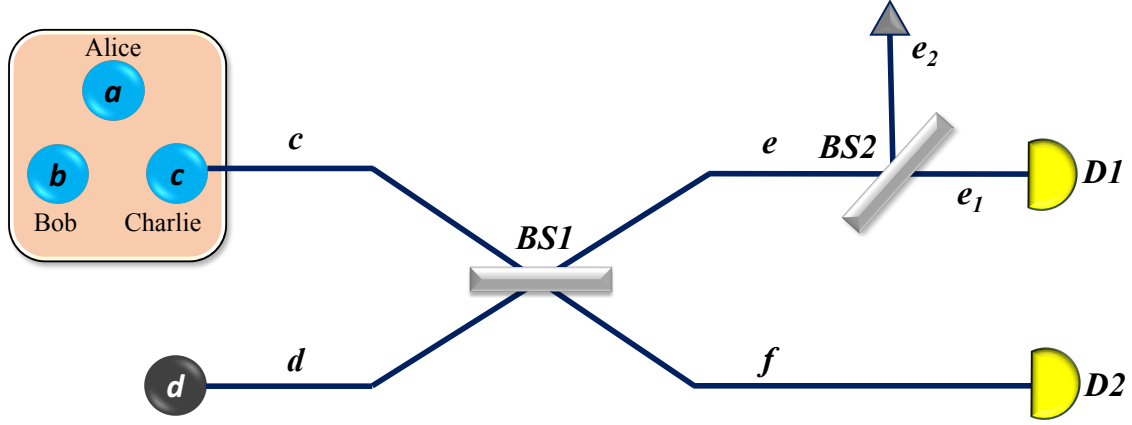


Figure 1: The schematic diagram of the proposed ECP for 3-mode GHZ-type ECS. Initially, Alice, Bob and Charlie share the spacial modes a , b , and c , respectively of a partially entangled coherent state $|\Psi'\rangle_{abc}$ as shown in Eq. 2. Charlie also prepares a single-mode coherent state in spatial mode d . Two beam splitters $BS1$ and $BS2$ and two detectors $D1$ and $D2$ have been used to perform the concentration protocol.

$$\begin{aligned}
|\xi\rangle_{abcd} &= |\Psi'\rangle_{abc} \otimes |\Phi\rangle_d \\
|\xi\rangle_{abcd} &= N_1 [\beta|\alpha\rangle_a|\alpha\rangle_b|\alpha\rangle_c + \gamma|-\alpha\rangle_a|-\alpha\rangle_b|-\alpha\rangle_c] \otimes N_2 [\gamma|\alpha\rangle_d + \beta|-\alpha\rangle_d] \\
|\xi\rangle_{abcd} &= N_1 N_2 [\beta\gamma|\alpha\rangle_a|\alpha\rangle_b|\alpha\rangle_c|\alpha\rangle_d + \beta^2|\alpha\rangle_a|\alpha\rangle_b|\alpha\rangle_c|-\alpha\rangle_d \\
&\quad + \gamma^2|-\alpha\rangle_a|-\alpha\rangle_b|-\alpha\rangle_c|\alpha\rangle_d + \gamma\beta|-\alpha\rangle_a|-\alpha\rangle_b|-\alpha\rangle_c|-\alpha\rangle_d].
\end{aligned} \tag{4}$$

Subsequently, they let the photons in spatial mode c and d pass through the 50:50 beam splitter (BS) denoted as $BS1$. The BS transforms two different coherent states $|\alpha\rangle$ and $|\beta\rangle$ to the states

$$BS|\alpha\rangle|\beta\rangle \rightarrow \left| \frac{\alpha + \beta}{\sqrt{2}} \right\rangle \left| \frac{\alpha - \beta}{\sqrt{2}} \right\rangle. \tag{5}$$

There are four different possibilities exist when the photons in spatial mode c and d incident onto the 50:50 BS . It can be described as

$$\begin{aligned}
BS|\alpha\rangle_c|\alpha\rangle_d &\rightarrow |\sqrt{2}\alpha\rangle_e|0\rangle_f, \\
BS|\alpha\rangle_c|-\alpha\rangle_d &\rightarrow |0\rangle_e|\sqrt{2}\alpha\rangle_f, \\
BS|-\alpha\rangle_c|\alpha\rangle_d &\rightarrow |0\rangle_e|-\sqrt{2}\alpha\rangle_f, \\
BS|-\alpha\rangle_c|-\alpha\rangle_d &\rightarrow |-\sqrt{2}\alpha\rangle_e|0\rangle_f.
\end{aligned} \tag{6}$$

Following Eq. 6, the photons in spatial mode c and d (of Eq. 4) pass through the $BS1$, then the Eq. 4 can be expressed as

$$\begin{aligned}
|\xi\rangle_{abef} &= N_1 N_2 [\beta\gamma|\alpha\rangle_a|\alpha\rangle_b|\sqrt{2}\alpha\rangle_e|0\rangle_f + \beta^2|\alpha\rangle_a|\alpha\rangle_b|0\rangle_e|\sqrt{2}\alpha\rangle_f \\
&\quad + \gamma^2|-\alpha\rangle_a|-\alpha\rangle_b|0\rangle_e|-\sqrt{2}\alpha\rangle_f + \gamma\beta|-\alpha\rangle_a|-\alpha\rangle_b|-\sqrt{2}\alpha\rangle_e|0\rangle_f].
\end{aligned} \tag{7}$$

It is evident in the above equation that the terms $|\alpha\rangle_a|\alpha\rangle_b|\sqrt{2}\alpha\rangle_e|0\rangle_f$, $|-\alpha\rangle_a|-\alpha\rangle_b|-\sqrt{2}\alpha\rangle_e|0\rangle_f$ and other terms $|\alpha\rangle_a|\alpha\rangle_b|0\rangle_e|\sqrt{2}\alpha\rangle_f$, $|-\alpha\rangle_a|-\alpha\rangle_b|0\rangle_e|-\sqrt{2}\alpha\rangle_f$ do not have photons in the spatial mode f and e , respectively. Therefore, they adopt the post selection method to choose those two terms where the spatial mode f has no photon and the modified state in Eq. 7 can be expressed (before normalization)

$$|\xi\rangle_{abe} = N_1 N_2 \left[\beta\gamma \left(|\alpha\rangle_a|\alpha\rangle_b|\sqrt{2}\alpha\rangle_e + |-\alpha\rangle_a|-\alpha\rangle_b|-\sqrt{2}\alpha\rangle_e \right) \right]. \tag{8}$$

We can find that the state in Eq. 8 has the same form with that in Eq. 1. However, the amplitude of Eq. 8 in mode e is $\sqrt{2}$ times larger than the Eq. 1 in spatial mode c , which can be seen as an advantage for long-distance quantum communication. Still, to obtain the desired maximally entangled 3-mode GHZ-type ECS as shown in Eq. 1, the coherent state in spatial mode e passes through $BS2$ and the state evolves to

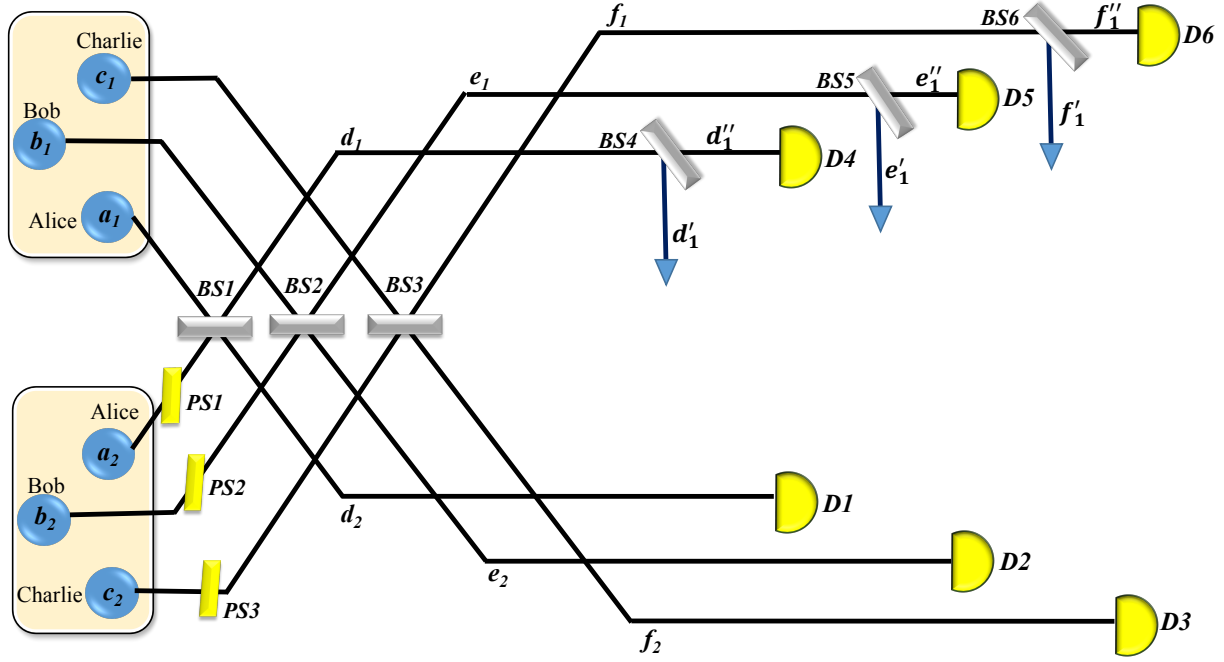


Figure 2: The schematic diagram of the proposed ECP for 3-mode GHZ-type ECS. First, Alice, Bob and Charlie share two copies of entangled coherent states denoted as a_1, b_1, c_1 and a_2, b_2, c_2 , respectively. Each of them performs a phase shift ($PS1 - PS3$) operation on the second pair (a_2, b_2, c_2). Six beam splitters $BS1 - BS6$ and six detectors $D1 - D6$ have been used to perform the concentration protocol.

$$|\xi\rangle_{abe_1e_2} = N_1 N_2 [\beta\gamma (|\alpha\rangle_a |\alpha\rangle_b |\alpha\rangle_{e_1} |\alpha\rangle_{e_2} + |-\alpha\rangle_a |-\alpha\rangle_b |-\alpha\rangle_{e_1} |-\alpha\rangle_{e_2})]. \quad (9)$$

To accomplish our ECP, Charlie performs the photon number measurement of the coherent state in the mode e_1 without distinguishing $|\pm\alpha\rangle$ and the state becomes

$$|\xi\rangle_{abe_2} = N_0 [|\alpha\rangle_a |\alpha\rangle_b |\alpha\rangle_{e_2} + |-\alpha\rangle_a |-\alpha\rangle_b |-\alpha\rangle_{e_2}]. \quad (10)$$

Finally, they get the desired maximally entangled 3-mode GHZ-type ECS which is of the form of Eq. 1 with success probability $P = 2(N_1 N_2 \beta \gamma)^2$.

3 ECP with two copies of partially entangled 3-mode GHZ-type ECSs

In this section, we have discussed how to obtain a maximally entangled 3-mode GHZ-type ECS in a conventional way, i.e., with the help of two copies of partially entangled 3-mode GHZ-type ECSs.

To begin with, Alice and Bob share two copies of partially entangled 3-mode GHZ-type ECSs according to Fig. 2, which are of the form

$$|\psi\rangle_{a_1 b_1 c_1} = N [\delta |\alpha\rangle_{a_1} |\alpha\rangle_{b_1} |\alpha\rangle_{c_1} + \eta |-\alpha\rangle_{a_1} |-\alpha\rangle_{b_1} |-\alpha\rangle_{c_1}], \quad (11)$$

and

$$|\psi\rangle_{a_2 b_2 c_2} = N [\delta |\alpha\rangle_{a_2} |\alpha\rangle_{b_2} |\alpha\rangle_{c_2} + \eta |-\alpha\rangle_{a_2} |-\alpha\rangle_{b_2} |-\alpha\rangle_{c_2}]. \quad (12)$$

First copy is in spatial mode a_1, b_1, c_1 while the second copy is in spatial mode a_2, b_2, c_2 . In Eqs. 11 and 12, $N = [\delta^2 + \eta^2 + 2\delta\eta e^{-6|\alpha|^2}]^{-\frac{1}{2}}$ represents the normalization coefficient, whereas we have considered δ and η are real numbers. Further, to initiate the concentration process, first Alice, Bob and Charlie perform a phase shift (PS) operation on their

respective modes a_2 , b_2 , and c_2 corresponding to the second copy in Eq. 12. Consequently, the state in spatial mode a_2 , b_2 , c_2 becomes

$$|\psi'\rangle_{a_2 b_2 c_2} = N [\eta|\alpha\rangle_{a_2}|\alpha\rangle_{b_2}|\alpha\rangle_{c_2} + \delta|-\alpha\rangle_{a_2}|-\alpha\rangle_{b_2}|-\alpha\rangle_{c_2}]. \quad (13)$$

The combined state $|\psi\rangle_{a_1 b_1 c_1}$ and $|\psi'\rangle_{a_2 b_2 c_2}$ can be expressed as

$$\begin{aligned} & |\chi\rangle_{a_1 b_1 c_1 a_2 b_2 c_2} \\ = & |\psi\rangle_{a_1 b_1 c_1} \otimes |\psi'\rangle_{a_2 b_2 c_2} \\ = & N [\delta|\alpha\rangle_{a_1}|\alpha\rangle_{b_1}|\alpha\rangle_{c_1} + \eta|-\alpha\rangle_{a_1}|-\alpha\rangle_{b_1}|-\alpha\rangle_{c_1}] \otimes N [\eta|\alpha\rangle_{a_2}|\alpha\rangle_{b_2}|\alpha\rangle_{c_2} + \delta|-\alpha\rangle_{a_2}|-\alpha\rangle_{b_2}|-\alpha\rangle_{c_2}] \\ = & N^2 [\delta\eta|\alpha\rangle_{a_1}|\alpha\rangle_{b_1}|\alpha\rangle_{c_1}|\alpha\rangle_{a_2}|\alpha\rangle_{b_2}|\alpha\rangle_{c_2} + \delta^2|\alpha\rangle_{a_1}|\alpha\rangle_{b_1}|\alpha\rangle_{c_1}|-\alpha\rangle_{a_2}|-\alpha\rangle_{b_2}|-\alpha\rangle_{c_2} \\ & + \eta^2|-\alpha\rangle_{a_1}|-\alpha\rangle_{b_1}|-\alpha\rangle_{c_1}|\alpha\rangle_{a_2}|\alpha\rangle_{b_2}|\alpha\rangle_{c_2} + \delta\eta|-\alpha\rangle_{a_1}|-\alpha\rangle_{b_1}|-\alpha\rangle_{c_1}|-\alpha\rangle_{a_2}|-\alpha\rangle_{b_2}|-\alpha\rangle_{c_2}]. \end{aligned} \quad (14)$$

Now, the spatial modes $a_1 a_2$, $b_1 b_2$ and $c_1 c_2$ will pass through the $BS1$, $BS2$ and $BS3$, respectively. Similar to Eq. 7, by following the Eq. 6 the state becomes

$$\begin{aligned} |\chi\rangle_{d_1 d_2 e_1 e_2 f_1 f_2} = & N^2 [\delta\eta|\sqrt{2}\alpha\rangle_{d_1}|0\rangle_{d_2}|\sqrt{2}\alpha\rangle_{e_1}|0\rangle_{e_2}|\sqrt{2}\alpha\rangle_{f_1}|0\rangle_{f_2} \\ & + \delta^2|0\rangle_{d_1}|\sqrt{2}\alpha\rangle_{d_2}|0\rangle_{e_1}|\sqrt{2}\alpha\rangle_{e_2}|0\rangle_{f_1}|\sqrt{2}\alpha\rangle_{f_2} \\ & + \eta^2|0\rangle_{d_1}|-\sqrt{2}\alpha\rangle_{d_2}|0\rangle_{e_1}|-\sqrt{2}\alpha\rangle_{e_2}|0\rangle_{f_1}|-\sqrt{2}\alpha\rangle_{f_2} \\ & + \delta\eta|-\sqrt{2}\alpha\rangle_{d_1}|0\rangle_{d_2}|-\sqrt{2}\alpha\rangle_{e_1}|0\rangle_{e_2}|-\sqrt{2}\alpha\rangle_{f_1}|0\rangle_{f_2}]. \end{aligned} \quad (15)$$

With the post selection method, they choose the items $|\sqrt{2}\alpha\rangle_{d_1}|0\rangle_{d_2}|\sqrt{2}\alpha\rangle_{e_1}|0\rangle_{e_2}|\sqrt{2}\alpha\rangle_{f_1}|0\rangle_{f_2}$ and $|-\sqrt{2}\alpha\rangle_{d_1}|0\rangle_{d_2}|-\sqrt{2}\alpha\rangle_{e_1}|0\rangle_{e_2}|-\sqrt{2}\alpha\rangle_{f_1}|0\rangle_{f_2}$ in which the spatial mode d_2, e_2 and f_2 have no photon. The state evolves to

$$\begin{aligned} |\chi\rangle_{d_1 e_1 f_1} = & N^2 [\delta\eta (|\sqrt{2}\alpha\rangle_{d_1}|\sqrt{2}\alpha\rangle_{e_1}|\sqrt{2}\alpha\rangle_{f_1} \\ & + |-\sqrt{2}\alpha\rangle_{d_1}|-\sqrt{2}\alpha\rangle_{e_1}|-\sqrt{2}\alpha\rangle_{f_1})]. \end{aligned} \quad (16)$$

The above equation is same as Eq. 1 with the only difference that the amplitude in modes d_1, e_1 and f_1 is amplified (an advantage in long-distance quantum communication) by $\sqrt{2}$ in comparison to modes a, b and c of Eq. 1. Therefore, as shown in Fig. 2, they use the beamsplitters $BS4$, $BS5$ and $BS6$ to pass the spatial mode d_1, e_1 and f_1 of $|\chi\rangle_{d_1 e_1 f_1}$, and the state evolved as

$$\begin{aligned} |\chi\rangle_{d'_1 d''_1 e'_1 e''_1 f'_1 f''_1} = & N^2 [\delta\eta (|\alpha\rangle_{d'_1}|\alpha\rangle_{d''_1}|\alpha\rangle_{e'_1}|\alpha\rangle_{e''_1}|\alpha\rangle_{f'_1}|\alpha\rangle_{f''_1} \\ & + |-\alpha\rangle_{d'_1}|-\alpha\rangle_{d''_1}|-\alpha\rangle_{e'_1}|-\alpha\rangle_{e''_1}|-\alpha\rangle_{f'_1}|-\alpha\rangle_{f''_1})]. \end{aligned} \quad (17)$$

Subsequently, in order to complete our ECP, Alice, Bob and Charlie perform the photon number measurement of their respective coherent state in the mode d''_1, e''_1 and f''_1 without distinguishing $|\pm\alpha\rangle$ and the state can be written as

$$|\chi\rangle_{d'_1 e'_1 f'_1} = N_0 [|\alpha\rangle_{d'_1}|\alpha\rangle_{e'_1}|\alpha\rangle_{f'_1} + |-\alpha\rangle_{d'_1}|-\alpha\rangle_{e'_1}|-\alpha\rangle_{f'_1}]. \quad (18)$$

The above equation is our desired state as shown in Eq. 1. Finally, they obtain the concentrated maximally entangled 3-mode GHZ-type ECS with the total success probability $P = 2(N^2\delta\eta)^2$.

4 Success probability

In the last two sections, we have discussed the two ECPs for partially entangled 3-mode GHZ-type ECS. According to our first and second ECP performed in Sec. 2 and Sec. 3, we can calculate the success probabilities $P = 2(N_1 N_2 \beta \gamma)^2$ and $P = 2(N^2 \delta \eta)^2$, respectively. Now, we have plotted both of these P in Fig. 3 (a) and (b) and discussed the variation of P with state parameters. Specifically, in Fig. 3 (a), variation of P with β has been shown for $\alpha = 0.5, 1$, and 2 , which manifests that the success probability P increases with the increase in α and reaches at the peak (maximum possible value) at a constant value of $\beta = 0.7$ for all values of α . In Fig. 3 (b), variation of P with δ has been shown for $\alpha = 0.5, 1$, and 2 , which reveals exactly the similar behaviors as in Fig. 3 (a), though, the peak value is more i.e., $P = 3$ for $\alpha = 0.5$ and $P = 4.9$ for $\alpha = 1$ than the case in Fig. 3 (a). However, for $\alpha = 2$, both Fig. 3 (a) and (b) are equivalent. Further, our first ECP is more simple and only Charlie needs to perform the operation. On the other hand, our second ECP has an advantage as it is more efficient than our first ECP for $\alpha < 2$. It is to be noted that Ref. [50] would also obtain the similar nature as we have shown in Fig. 3.

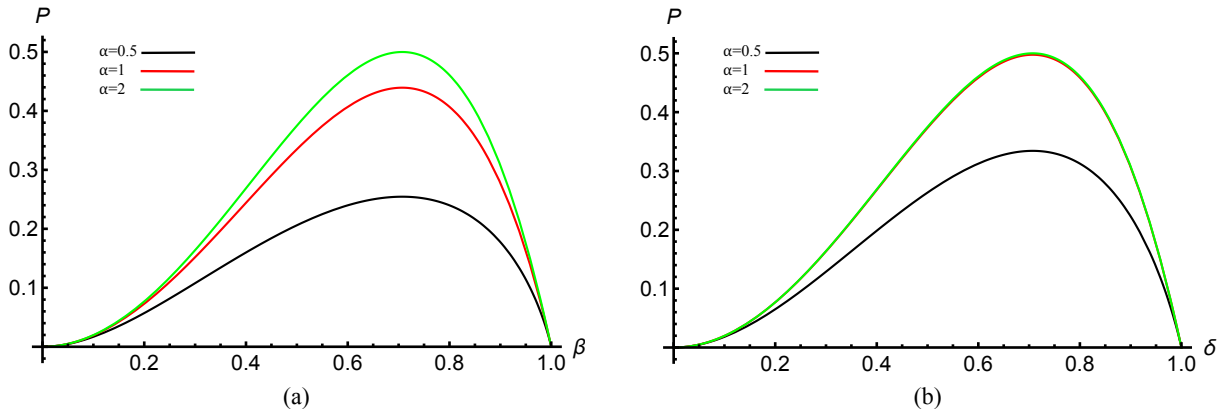


Figure 3: (Color online) Variation of success probability (P) to obtain a maximally entangled 3-mode GHZ-type ECS. (a) The variation of P with the coefficient β , (b) The variation of P with the coefficient δ , assuming $\alpha = 0.5, 1$, and 2 .

Furthermore, as there are two non-equivalent classes for 3-qubit entangled states i.e., GHZ class and W class [26], so it would be interesting to compare the success probabilities P of our first ECP (Sec. 2) for 3-mode GHZ-type ECS as shown in Fig. 3 (a) with 3-mode W-type ECS proposed in Sec. 2 and its corresponding Fig. 3 of [51]. It is worth mentioning that our ECP for 3-mode GHZ-type ECS exhibits maximal P at $\beta = 0.7$ for $\alpha = 0.5, 1$ and 2 . However, for 3-mode W-type ECS [51] P reaches at the maximal value at $\gamma = 0.5$ for $\alpha = 0.5$ and at $\gamma = 0.65$ for $\alpha = 1, 2$.

Although for $\alpha = 0.5$, our ECP for 3-mode GHZ-type ECS has slightly less maximal value ($P = 2.5$) than for 3-mode W-type ECS [51] maximal value ($P = 3$), however, our ECP has peak for larger value of $\beta = 0.7$ than for [51] which has peak for $\gamma = 0.5$. Similarly for $\alpha = 1$, our ECP for 3-mode GHZ-type ECS has slightly less maximal value ($P = 4.5$) than for 3-mode W-type ECS [51] maximal value ($P = 4.8$), however, our ECP has peak for larger value of $\beta = 0.7$ than for [51] which has peak for $\gamma = 0.64$. Subsequently for $\alpha = 2$, our ECP for 3-mode GHZ-type ECS has the same maximal value ($P = 5$) as for 3-mode W-type ECS [51] maximal value ($P = 5$), however, our ECP has peak for larger value of $\beta = 0.7$ than for [51] which has peak for $\gamma = 0.63$. Therefore, our ECP for 3-mode GHZ-type ECS as shown in Fig. 3 (a) is more efficient (has maximal P values) for larger values of state parameter than for 3-mode W-type ECS shown in Fig. 3 of [51].

5 Conclusion

Many quantum communication and technology applications which also have been mentioned in the introduction section, require distributed (shared) entanglement (maximal) that degrades due to decoherence while processing, manipulating and storing the quantum systems. Hence the degraded entanglement needs to be enhanced, however, it cannot be increased by local operation and classical communication. Consequently, Alice and Bob usually share a mixed entangled state which results in the fidelity less than unity. The only solution to this is to perform an ECP/EPP prior to start any quantum communication or computation task.

Here, we aim to propose the ECPs for 3-mode GHZ-type ECS for its use in the various applications proposed in the past [45] and in recent years [55, 56]. Basically, the development of ECSs based applications [57–59] are dependent on the proposal of the corresponding ECPs so that their physical realization can take place with unit success probability. On account of the importance of such CV applications, we have proposed two ECPs. In Sec. 2, the first ECP uses a superposition of single-mode coherent state and in Sec. 3 the second ECP uses the conventional way requiring the two copies of partially entangled 3-mode GHZ-type ECSs to obtain the concentrated maximally entangled 3-mode GHZ-type ECS. Further, we have discussed their success probabilities P in detail and later we have compared the success probabilities of our first ECP for 3-mode GHZ-type ECS with an ECP of 3-mode W-type ECS and found that our ECP is more efficient (maximal success probabilities) for larger value ($\beta = 0.7$) of state parameter. Finally, we have concluded our work with the expectation that our ECPs can be implemented experimentally in the near future for long-distance quantum communication or computation tasks.

Acknowledgments: MS thanks to the Department of Science and Technology (DST), India, for support provided through the DST project No. S/DST/VNA/20190004. Authors also thank Kishore Thapliyal for his interest in the work and helpful suggestions.

References

- [1] Bennett, C.H., Brassard, G., Crépeau, C., et al.: Teleporting an unknown quantum state via dual classical and Einstein–Podolsky–Rosen channels. *Phys. Rev. Lett.* **70**, 1895-1899 (1993)
- [2] Bennett, C.H., Wiesner, S.J.: Communication via one- and two-particle operators on Einstein-Podolsky-Rosen states. *Phys. Rev. Lett.* **69**, 2881-2884 (1992)
- [3] Ekert, A.K.: Quantum cryptography based on Bell’s Theorem. *Phys. Rev. Lett.* **67**, 661 (1991)
- [4] Shukla, C., Alam, N., Pathak, A.: Protocols of quantum key agreement solely using Bell states and Bell measurement. *Quantum Inf. Process.* **13**, 2391 (2014)
- [5] Shukla, C., Thapliyal, K., Pathak, A.: Semi-quantum communication: protocols for key agreement, controlled secure direct communication and dialogue. *Quantum Inf. Process.* **16**, 295 (2017)
- [6] Hillery, M., Bužek, V., Berthiaume, A.: Quantum secret sharing. *Phys. Rev. A* **59**, 1829-1834 (1999)
- [7] Shukla, C., Pathak, A.: Hierarchical quantum communication. *Phys. Lett. A* **377**, 1337–1344 (2013)
- [8] Shukla, C., Thapliyal, K., Pathak, A.: Hierarchical joint remote state preparation in noisy environment. *Quantum Inf. Process.* **16**, 205 (2017)
- [9] Bich, C.T., An, N.B.: Hierarchically controlling quantum teleportations. *Quantum Info. Process.* **18**, 245 (2019)
- [10] Long, G.-L., Deng, F.-G., Wang, C., Li, X.-h., Wen, K., Wang, W.-y.: Quantum secure direct communication and deterministic secure quantum communication. *Front. Phys. China* **2**, 251 (2007)
- [11] Shukla, C., Banerjee, A., Pathak, A., Srikanth, R.: Secure quantum communication with orthogonal states. *Int. J. Quantum Inf.* **14**, 1640021 (2016)
- [12] Pathak, A.: *Elements of Quantum Computation and Quantum Communication*. CRC Press, Boca Raton (2013)
- [13] Li, W.-L., Li, C.-F., Guo, G.-C.: Probabilistic teleportation and entanglement Matching. *Phys. Rev. A* **61**, 034301 (2000)
- [14] Nielsen, M.A., Chuang, I.L., *Quantum Computation and Quantum Information* (Cambridge: Cambridge University Press) (2000)
- [15] Bennett, C.H., Bernstein, H.J., Popescu, S., Schumacher, B.: Concentrating partial entanglement by local operations. *Phys. Rev. A* **53**, 2046-2052 (1996)
- [16] Bose, S., Vedral, V., Knight, P.L.: Purification via entanglement swapping and conserved entanglement. *Phys. Rev. A* **60**, 194-197 (1999)
- [17] Sheng, Y.-B., Zhou, L., Zhao, S.-M., Zheng, B.-Y.: Efficient single-photon-assisted entanglement concentration for partially entangled photon pairs. *Phys. Rev. A* **85**, 012307 (2012)
- [18] Zhao, S.Y., Liu, J., Zhou, L., Sheng, Y.B.: Two-step entanglement concentration for arbitrary electronic cluster state. *Quantum Inf. Process.* **12**, 3633 (2013)
- [19] Zhao, Z., Pan, J.-W., Zhan, M.S.: Practical scheme for entanglement concentration. *Phys. Rev. A* **64**, 014301 (2001)
- [20] Shukla, C., Banerjee, A., Pathak, A.: Protocols and quantum circuits for implementing entanglement concentration in cat state, GHZ-like state and 9 families of 4-qubit entangled states. *Quantum Inf. Process.* **14**, 2077 (2015)
- [21] Du, F.F., Long, G.L.: Refined entanglement concentration for electron-spin entangled cluster states with quantum-dot spins in optical microcavities. *Quantum Inf. Process.* **16**, 26 (2017)
- [22] Liu, J., Zhou, L., Zhong, W., Sheng, Y.-B.: Logic Bell state concentration with parity check measurement. *Front. Phys.* **14**, 21601 (2019)
- [23] Wang, X., Hu, Z.-N.: Entanglement concentration for photon systems assisted with single photons. *Optik - Int. J. Light and Electron Optics* **176**, 143-151 (2019)

- [24] Wang, X., Hu, Z.-N.: Entanglement concentration for photon systems assisted with single photons. *Optik-Int. J. for Light and Electron Optics* **176**, 143-151 (2019)
- [25] Zhao, Z., Yang, T., Chen, Y.-A., Zhang, A.-N., Pan, J.-W.: Experimental realization of entanglement concentration and a quantum repeater. *Phys. Rev. Lett.* **90**, 207901 (2003)
- [26] Cunha, M.M., Fonseca, A., Silva, E.O.: *Tripartite Entanglement: Foundations and Applications*. Universe, **5**, 209 (2019)
- [27] Xia, Y., Hao, S.-Y., Dong, Y.-J., Song, J.: Effective schemes for preparation of Greenberger–Horne–Zeilinger and W maximally entangled states with cross-Kerr nonlinearity and parity-check measurement. *Applied Physics B* **110**, 551-561 (2013)
- [28] Tsujimoto, Y., Tanaka, M., Iwasaki, N., Ikuta, R., Miki, S., Yamashita, T., Terai, H., Yamamoto, T., Koashi, M., Imoto, N.: High-fidelity entanglement swapping and generation of three-qubit GHZ state using asynchronous telecom photon pair sources. *Scientific Reports* **8**, 1446 (2018)
- [29] Zhang, C., Huang, Y.-F., Wang, Z., Liu, B.-H., Li, C.-F., Guo, G.-C.: Experimental Greenberger-Horne-Zeilinger-Type six-photon quantum nonlocality. *Phys. Rev. Lett.* **115**, 260402 (2015)
- [30] Ren, C., Su, H.-Y., Xu, Z.-P., Wu, C., Chen, J.-L.: Optimal GHZ paradox for three qubits. *Scientific Reports* **5**, 13080 (2015)
- [31] Quan, Q., Zhao, M.-J., Fei, S.-M., Fan, H., Yang, W.-L., Wang, T.-J., Long, G.-L.: Two-copy quantum teleportation based on GHZ measurement. *Quantum Inf. Process.* **19**, 205 (2020)
- [32] Zhang, H., Wang, H.: Entanglement concentration of microwave photons based on the Kerr effect in circuit QED. *Phys. Rev. A* **95**, 052314 (2017)
- [33] Deng, F.G.: Optimal nonlocal multipartite entanglement concentration based on projection measurements. *Phys. Rev. A* **85**, 022311 (2012)
- [34] Chen, S.-S., Zhang, H., Ai, Q., Yang, G.-J.: Phononic entanglement concentration via optomechanical interactions. *Phys. Rev. A* **100**, 052306 (2019)
- [35] Sanders, B.C.: Entangled coherent states. *Phys. Rev. A* **45**, 6811 (1992)
- [36] Sanders, B.C.: Review of entangled coherent states. *J. Phys. A: Math. Theor.* **45**, 244002 (2012)
- [37] Su, X., Tan, A., Jia, X., Zhang, J., Xie, C., Peng, K.: Experimental preparation of quadripartite cluster and Greenberger-Horne-Zeilinger entangled states for continuous variables. *Phys. Rev. Lett.* **98**, 070502 (2007)
- [38] Yukawa, M., Ukai, R., van Loock, P., Furusawa, A.: Experimental generation of four-mode continuous-variable cluster states. *Phys. Rev. A* **78**, 012301 (2008)
- [39] Jeong, H., An, N.B.: Greenberger-Horne-Zeilinger-type and W-type entangled coherent states: Generation and Bell-type inequality tests without photon counting. *Phys. Rev. A* **74**, 022104, (2006)
- [40] An, N.B., Kim, J.: Cluster-type entangled coherent states: generation and application. *Phys. Rev. A* **80**, 042316 (2009)
- [41] Chen, H.N., Liu, J.M.: Teleportation of a bipartite entangled coherent state via a four-partite cluster-type entangled state. *Commun. Theor. Phys.* **52**, 597-600 (2009)
- [42] Luiz, F.S., Rigolin, G.: Teleportation-based continuous variable quantum cryptography. *Quantum Inf. Process.* **16**, 58 (2017)
- [43] Wang, X.: Quantum teleportation of entangled coherent states. *Phys. Rev. A* **64**, 022302 (2001)
- [44] Prakash, H., Chandra, N., Prakash, R., Shivani: Improving the teleportation of entangled coherent states. *Phys. Rev. A* **75**, 044305 (2007)
- [45] Allati, A. El, Baz, M. El, Hassouni, Y.: Quantum key distribution via tripartite coherent states. *Quantum Inf. Process.* **10**, 589-602 (2011)

- [46] Menicucci, N.C., Loock, P.v., Gu, M., Weedbrook, C., Ralph, T.C., Nielsen, M.A.: Universal quantum computation with continuous-variable cluster states. *Phys. Rev. Lett.* **97**, 110501 (2006)
- [47] Gu, M., Weedbrook, C., Menicucci, N.C., Ralph, T.C., Loock, P.V.: Quantum computing with continuous-variable clusters. *Phys. Rev. A* **79**, 062318 (2009)
- [48] Weedbrook, C., Pirandola, S., García-Patrón, R., Cerf, N.J., et.al.: Gaussian quantum information. *Rev. Mod. Phys.* **84**, 621 (2012)
- [49] An, N.B.: Optimal processing of quantum information via W-type entangled coherent states. *Phys. Rev. A* **69**, 022315 (2004)
- [50] Sheng, Y.-B., Qu, C.-C., Yang, O.-Y., Feng, Z.-F., Zhou, L.: Practical Entanglement Concentration for Entangled Coherent States. *Int. J. of Theor. Phys.* **53**, 2033-2040 (2014)
- [51] Sheng, Y.-B., Liu, J., Zhao, S.-Y., Wang, L., Zhou, L.: Entanglement concentration for W-type entangled coherent states. *Chin. Phys. B* **23**, 080305 (2014)
- [52] Sisodia, M., Shukla, C., Long, G.L.: Linear optics-based entanglement concentration protocols for cluster-type entangled coherent state. *Quantum Inf. Process.* **18**, 253 (2019)
- [53] Guo, R., Zhou, L., Gu, S.-P., Wang, X.-F., Sheng, Y.-B.: Hybrid entanglement concentration assisted with single coherent state. *Chin. Phys. B* **25**, 030302 (2016)
- [54] Shukla, C., Malpani, P., Thapliyal, K.: Hybrid Entanglement concentration and its application in hierarchical quantum teleportation network. *arXiv:2004.13176v2 [quant-ph]* (2020)
- [55] Pandey, R.K., Prakash, R., Prakash, H.: Controlled quantum teleportation of superposed coherent state using GHZ entangled coherent state. *Int. J. Theor. Phys.* **58**, 3342-3351 (2019)
- [56] Prakash, R., Pandey, R.K., Prakash, H.: Controlled entanglement diversion using GHZ type entangled coherent state. *Int. J. Theor. Phys.* **58**, 1227-1236 (2019)
- [57] Wang, X.: Quantum teleportation of entangled coherent states. *Phys. Rev. A* **64**, 022302 (2001)
- [58] van Enk, S.J., Hirota, O.: Entangled coherent states: Teleportation and decoherence. *Phys. Rev. A* **64**, 022313 (2001)
- [59] van Enk, S.J.: Entanglement capabilities in infinite dimensions: multidimensional entangled coherent states. *Phys. Rev. Lett.* **91**, 017902 (2003)